The Influence of Applied Stress Ratio on Fatigue Strength of TiN-coated Carbon Steel*

Kazuaki SHIOZAWA**, Seiichi NISHINO**
and Keiichi HANDA***

The influence of applied stress ratio on the fatigue strength of carbon steel coated with TiN was studied on the basis of measurement of crack initiation with the D. C. potential method. Fatigue tests were performed under the stress ratios of $R=0$ and -1 in air using the round notched specimens of 0.37%C steel, JIS S35C, normalized and coated with TiN by physical vapor deposition (PVD) and chemical vapor deposition (CVD). From the experimental results, increase in fatigue strength was observed in TiN-coated specimens under test conditions of $R=-1$, as compared with that of uncoated specimens. However, the fatigue life of specimens coated by PVD was decreased under the tests of $R=0$, except for the region of low stress amplitude. Also, the fatigue life of specimens coated by CVD under test conditions of $R=0$ was smaller than that of uncoated specimens. The difference in fatigue life with applied stress ratio is explained by the fracture behavior of coating film on the specimen surface.

Key Words: Fatigue, TiN-coated Carbon Steel, Physical Vapor Deposition, Chemical Vapor Deposition, D.C. Potential Method, Crack Initiation, Stress Ratio

1. Introduction

It is well known that the coating of TiN or TiC applied by physical vapor deposition (PVD) or chemical vapor deposition (CVD) for various kinds of machine components improves the wear resistance, cutting ability or cavitation-erosion resistance. TiN-coated metal will be utilized more widely for various kinds of machine components and structures which require high wear resistance.

One of the authors has previously reported that fatigue life of TiN-coated carbon steel increased in air[1] and in 3% saline solution[2] as compared with an uncoated specimen. This is due to the fact that TiN coating film improves crack initiation life in air, and protects the substrate from the corrosive environment. In contrast, there have been some studies on the rules of surface coating which govern the effects on fatigue life. These investigations on the fatigue of steels coated with TiN or TiC by PVD or CVD have reported fatigue lifetimes to be increased[3], decreased[4] or sometimes unaffected by the residual stresses in the surface layer and substrate, the hardness of the coating film, structural changes in the substrate with coating treatment, and the fracture behavior of the coating film during the fatigue process. The various mechanisms by which ceramics coatings can affect the fatigue behavior have yet to be documented in any systematic way. The aim of this investigation is to clarify the fatigue behavior of steel coated with TiN by PVD or CVD, in order to apply the process of ceramics coating to machine components and structures.

In this study, fatigue tests were conducted under the stress ratios of $R=0$ and $R=-1$ using specimens of 0.37% carbon steel coated with TiN by PVD and CVD, in order to study the influence of applied stress ratio on the fatigue strength. In order to observe the crack initiation, we employed the replica and D.C. potential methods.

* Received 13th November, 1991. Paper No. 90-1286 A
** Faculty of Engineering, Toyama University, 3190 Gofuku, Toyama 930, Japan
*** Kawasaki Heavy Industries, LTD., 2-1-8 Wadayamadori, Hyogo-ku, Kobe 652, Japan

2. Experimental Procedure

2.1 Testing material and coating conditions

The substrate material used in this investigation was 0.37% carbon steel, JIS S35C, normalized at 1 138 K for 30 min. Table 1 lists the chemical composition of this steel. Specimens were smooth bars with a 10 mm diameter and 100 mm gauge length for the static tensile test, and round notched bars with a minimum diameter of 8 mm, of which the stress concentration factor is 1.5 for fatigue tests, as shown in Fig. 1. Before TiN deposition, the substrates were polished with emery paper (grade # 1000) and electropolished to a depth of about 15 μm.

TiN coating was deposited onto the specimen surface by use of PVD and CVD processes. In PVD coating, the hollow cathode discharge process was employed In vacuum to generate a glow discharge in nitrogen into which titanium was evaporated at a constant substrate temperature of 623 K. Its thickness was 2-3 μm and Vickers hardness was H_V (15 gf) 1888.

Figure 2 shows the CVD coating process. In CVD coating, specimens were inserted into a stream of mixed gases of H_2-N_2-$TiCl_4$ under a reduced pressure of 3.37×10^3Pa at 1 223 K or 1 273 K for 3 hours. Thickness and Vickers hardness of CVD-coated layers were 5-6 μm and H_V (50 gf) 2 170, respectively.

Figure 3 shows the microstructure of TiM-coated material. The substrate of PVD coating is similar in structure to the uncoated one, which has ferrite and pearlite structure. On the other hand, the ferrite and pearlite structure of the CVD specimen is larger than that of the uncoated one. This is due to the high temperature during the CVD coating process. Also, decarburization of the substrate near the TiN layer of CVD coating (1 223 K) was observed[1].

Table 1 Chemical composition of JIS S35C (wt.%)

C	Si	Mn	P	S	Cu	Ni	Cr
0.37	0.24	0.77	0.019	0.023	0.1	0.2	0.4

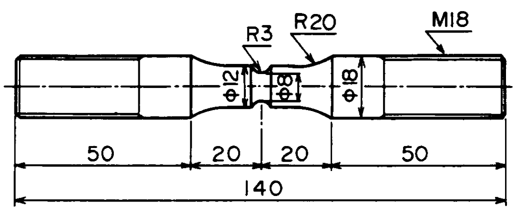

Fig. 1 Shape and dimensions of fatigue test specimen

2.2 Testing method

Two types of fatigue tests were performed under stress controlled conditions in air using the electro-hydraulic fatigue testing machine operated at a frequency of 20Hz; the two stress ratios used were $R=\sigma_{min}/\sigma_{max}=0$ and $R=-1$.

The D.C. potential method was employed to observe crack initiation in the substrate. A constant current of 10 A was supplied to the specimen, and the electric potential between the edges of the round notch was detected by digital potentiometer, for which resolution was 0.1 μV. Electric potential during fatigue was measured by reducing the frequency to 0.1 Hz. Cracks on the specimen surface were measured by optical microscope on the replicas which were taken from the specimen surface, at various intervals during

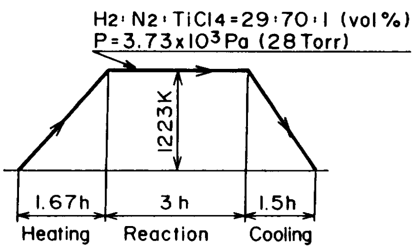

(a) 1223 K

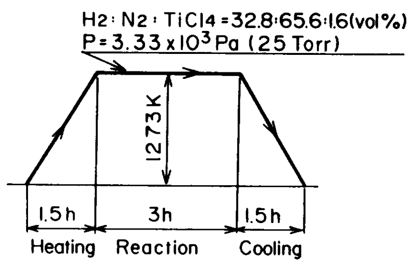

(b) 1273 K

Fig. 2 Schematic diagram of CVD method

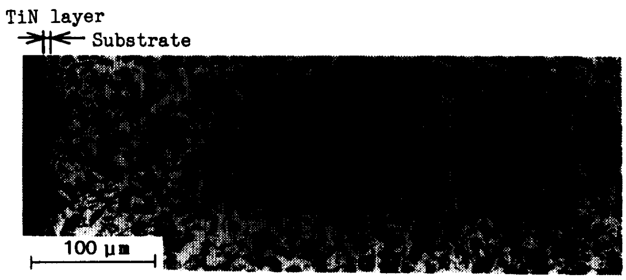

(a) PVD

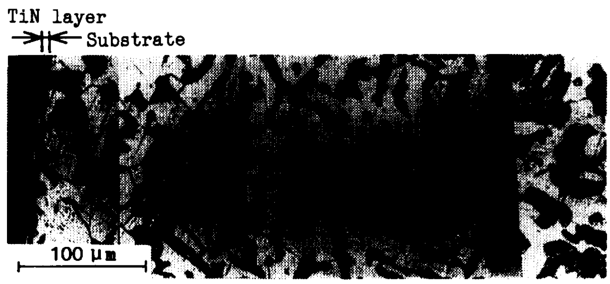

(b) CVD (1223 K)

Fig. 3 Microstructure of TiN-coated material

Table 2 Mechanical property of the tested materials

Material	Upper yield stress σ_{SU} (MPa)	Lower yield stress σ_{SL} (MPa)	Tensile strength σ_B (MPa)	Young's modulus E (GPa)	Elongation δ (%)	Area reduction ϕ (%)	Vickers Hardness Hv (100gf)
No coating (S35C, Normalizing)	401	371	616	204	25.8	60.1	215
PVD coating	389	354	615	206	25.1	63.2	220
CVD coating (1223K)	316	295	580	204	24.0	51.4	196
CVD coating (1273K)	299	293	606	195	27.0	46.7	197

(a) ε=0.43%

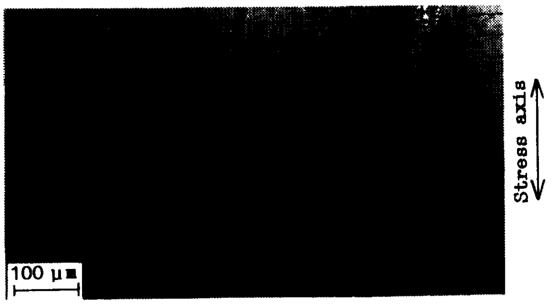

(b) ε=1.49%

Fig. 4 Typical examples of flaw on TiN coating film by PVD

fatigue life. Also, cyclic deformation behavior of the specimen was measured by extensometer.

3. Experimental Results and Discussion

3.1 Static tensile tests

Table 2 shows the results of static tensile tests and the hardness of the substrate. From the results of static tensile tests, PVD-coated material has the same mechanical properties as those of uncoated material. Thus, the TiN layer coated by PVD does not affect the mechanical property of the material. However, the yield stress and hardness of CVD-coated material decreased significantly as compared with those of uncoated and PVD-coated material, because the microstructure of the substrate was changed during the CVD process.

Figure 4 shows the flaws on the coating film obtained from observation by optical microscope of

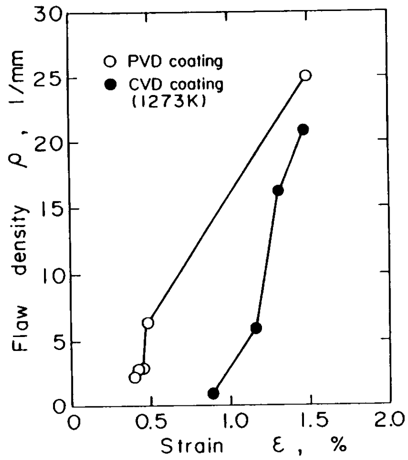

Fig. 5 Relation between flaw density on TiN coating film and total tensile strain

the replicas which were taken from the surface at various strains during the tensile test. Flaws of the coating film were perpendicular to the stress axis, and density increased with the strain.

Figure 5 shows the experimental relation between flaw density on the coating film and total tensile strain of the specimen, where flaw density was defined as the number of flaws per millimeter along the axial direction. It was found that flaws on PVD and CVD coating films occurred at the total tensile strains of 0.40% and 0.87%, respectively, and that they increased with the strain.

3.2 Fatigue tests

Figure 6 shows the experimental results obtained from the fatigue tests conducted under the condition of a stress ratio of $R=0$. It can be seen from this figure that the fatigue life of specimens coated by PVD increased in the region of the stress range below about 390 MPa, as compared with that of the uncoated one. On the other hand, fatigue life decreased for the region in the high-stress range. It is speculated that cyclic deformation behavior of the specimen affects the fatigue strength, because the value of the stress range (390 MPa) is similar to the yield stress for the

PVD-coated specimen. The results of the measurement of cyclic deformation behavior of the specimen will be described later. The fatigue limit of PVD-coated specimens increased about 11%, as compared with uncoated ones. Fatigue strength of specimens coated by CVD decreased significantly as compared with that of uncoated specimens.

Figure 7 shows experimental results obtained from the fatigue tests performed under the condition of a stress ratio of $R=-1$. It can be seen from this figure that fatigue strength of coated specimens increased under all of the stress amplitude levels, as compared with that of uncoated specimens, and in contrast to the experimental results mentioned above. About 18% and 4% increases in fatigue limit were observed in PVD- and CVD- coated specimens, respectively, as compared with uncoated specimens. In Fig. 7, the experimental results obtained from the tests using the specimen with the CVD coating film removed by electropolish, are also shown. Fatigue strength of this specimen is smaller than that of the uncoated specimen, because of structural change due to the high temperature used in the CVD coating process. To discuss the effect of CVD coating film on the fatigue strength, it is reasonable to compare the results obtained from the specimen coated by CVD with those treated at the same temperature by the CVD process. From this point of view, the fatigue limit of CVD-coated specimens is improved about 37% as compared with that of specimens with the coating film removed.

3.3 Cyclic deformation behavior

In order to discuss the effects of stress ratio and stress level, cyclic deformation behavior of the specimen was measured by extensometer. Figure 8 shows the variation in cyclic deformation of PVD- and CVD-coated specimens. It can be seen from these figures that displacement between the edge of the notch increased during the fatigue process under testing conditions where $R=0$ and at $2\sigma_a$ above 390 MPa of PVD and CVD, which were the conditions where fatigue strength decreased. On the other hand, under testing conditions where $R=0$ and at $2\sigma_a$ below 390 MPa and $R=-1$, which were the conditions where fatigue strength increased, the displacement did not increase. From these results, it is clear that fatigue strength of coated specimens depends on deformation behavior and is closely related to flaws in the coating film, because flaw on the coating film occur at small strain levels.

3.4 Crack initiation and propagation behavior

In order to discuss crack initiation and propagation behavior, the replica and D.C. potential methods were employed. Figure 9 shows the results from the

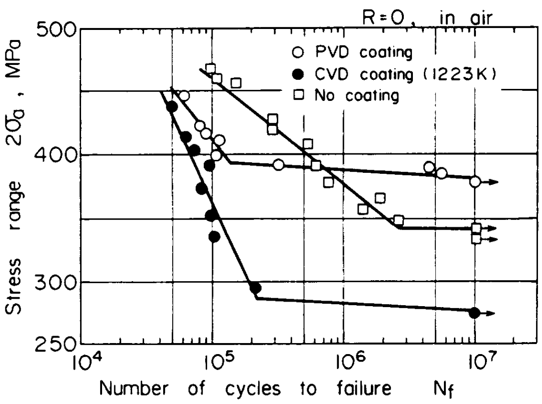

Fig. 6 S-N diagram under $R=0$ in air

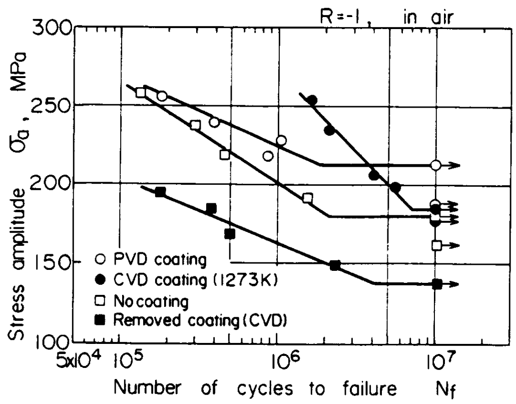

Fig. 7 S-N diagram under $R=-1$ in air

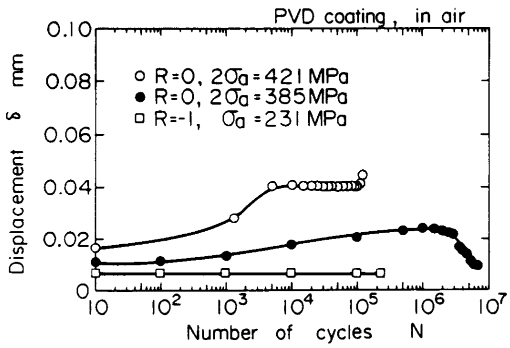

(a) PVD

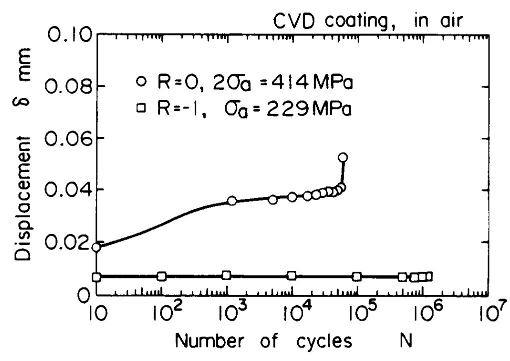

(b) CVD

Fig. 8 Variation in deformation during fatigue observation of replicas which were taken from the specimen surface during fatigue. The flaws in PVD coating films are perpendicular to the stress axis, and density increased with the fatigue process. In CVD coating, the flaw initiation and propagation behavior was similar to that of PVD coating, and density was larger than that of the PVD coating film.

Figure 10 shows the variation in potential ratio E/E_0 during the fatigue process, where E_0 is an average value of the potential in the first 10 cycles, and the arrows in these figures show the number of cycles to crack initiation, obtained from the observations of replicas. It can be seen from Fig. 10(a) that E/E_0 increased after the cycle of crack initiation. Thus, the variation in E/E_0 is correlated with crack initiation and propagation behavior. Figures 10(b) and (c) show the variation in E/E_0 of coated specimens under testing conditions of stress ratios of $R=0$ and $R=-1$, respectively. It can be seen from Fig. 10(b) that E/E_0 increased before the crack initiation of the uncoated specimen, except under testing conditions where $2\sigma_a=$ 385 MPa of PVD. Under the former conditions, fatigue strength decreased and under the latter conditions, fatigue strength increased. In Fig. 10(c), E/E_0 of coated specimens increased after the cycle of crack initiation of the uncoated specimen; in this case, fatigue strength increased. It can be seen from these

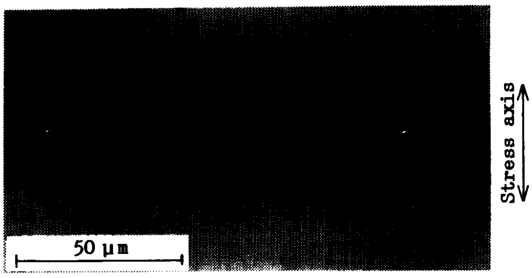

(a) PVD ($R=0$, $2\sigma_a=421$ MPa, $N/N_f=8\text{X}10^{-5}$)

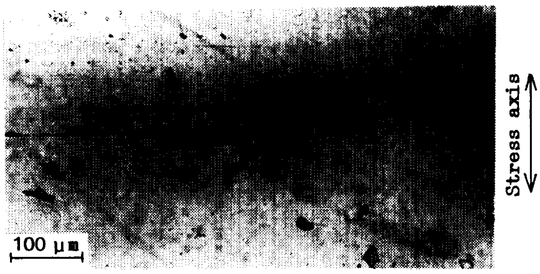

(b) PVD ($R=0$, $2\sigma_a=421$ MPa, $N/N_f=0.92$)

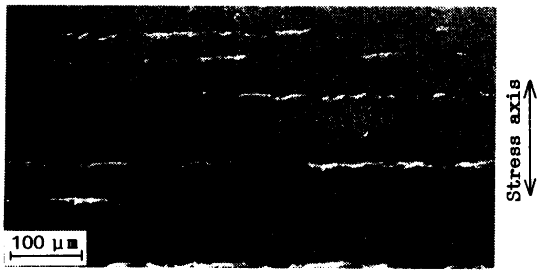

(c) CVD ($R=0$, $2\sigma_a=414$ MPa, $N/N_f=2\text{X}10^{-4}$)

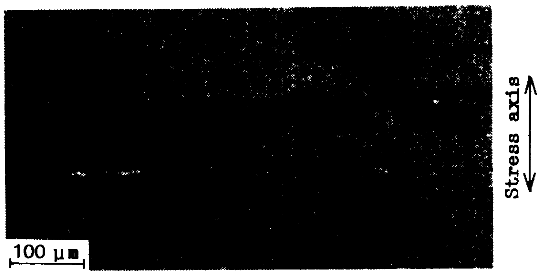

(d) CVD ($R=0$, $2\sigma_a=414$ MPa, $N/N_f=0.95$)

Fig. 9 Typical examples of flaws on TiN coating film during fatigue

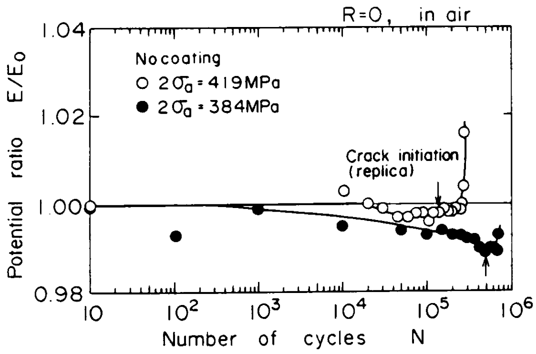

(a) $R=0$, Nocoating

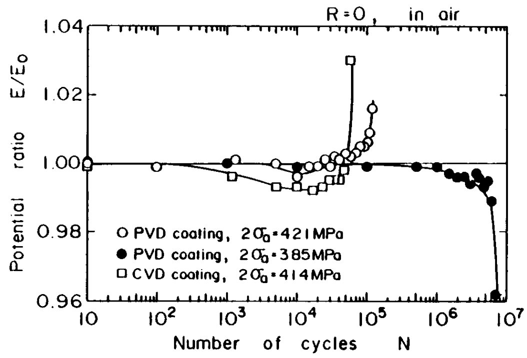

(b) $R=0$, TiN-coated carbon steel

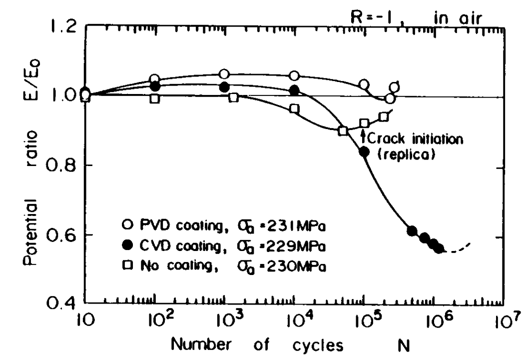

(c) $R=-1$, Nocoating and TiN-coated carbon steel

Fig. 10 Variation in potential ratio, E/E_0, during fatigue results that in the case of decreased fatigue strength of coated specimens, the number of cycles to crack initiation was decreased by the coating film. On the other hand, in the case of increased fatigue strength, crack initiation was delayed by the coating film.

Tables 3 and 4 show the number of cycles to crack initiation, N_i, number of cycles for crack propagation, N_p, $(N_p = N_f - N_i)$, and number of cycles to failure N_f, where N_i was defined from the variation in E/E_0, according to the recommendation method by the Iron and Steel Institute of Japan[5]. The values of N_i of PVD-coated specimens at a stress range of 419 MPa and CVD-coated specimens were smaller than those of uncoated specimens. However, the value of N_i of the PVD-coated specimen at 385 MPa was larger than that of the uncoated specimens. Also, N_p of the coated specimen was similar to that of the uncoated specimens. It can be seen from these results that the TiN coating on the specimen surface affects the crack initiation behavior but does not affect the crack propagation behavior.

Table 3 N_i, N_p and N_f obtained by the D. C. potential method $(R=0)$

Material	$2\sigma_a$ (MPa)	N_i (N_i/N_f)	N_p (N_p/N_f)	N_f
No coating (S35C, Normalizing)	419	1.40×10^5 (0.49)	1.48×10^5 (0.51)	2.88×10^5
	384	4.90×10^5 (0.66)	2.58×10^5 (0.34)	7.48×10^5
PVD coating	421	1.50×10^4 (0.11)	1.16×10^5 (0.89)	1.31×10^5
	385	$>7.03\times10^6$ (>0.92)	$<6.30\times10^5$ (<0.08)	7.66×10^6
CVD coating (1223K)	414	2.32×10^4 (0.37)	3.90×10^4 (0.63)	6.22×10^4

Table 4 N_i, N_p and N_f obtained by the D.C. potential method $(R=-1)$

Material	σ_a (MPa)	N_i (N_i/N_f)	N_p (N_p/N_f)	N_f
No coating (S35C, Normalizing)	230	1.00×10^5 (0.51)	0.96×10 (0.49)	1.96×10^5
PVD coating	231	2.34×10^5 (0.84)	0.44×10^5 (0.16)	2.78×10^5
CVD coating (1273K)	229	$>1.21\times10^6$ (>0.95)	$<0.70\times10^5$ (<0.05)	1.28×10^6

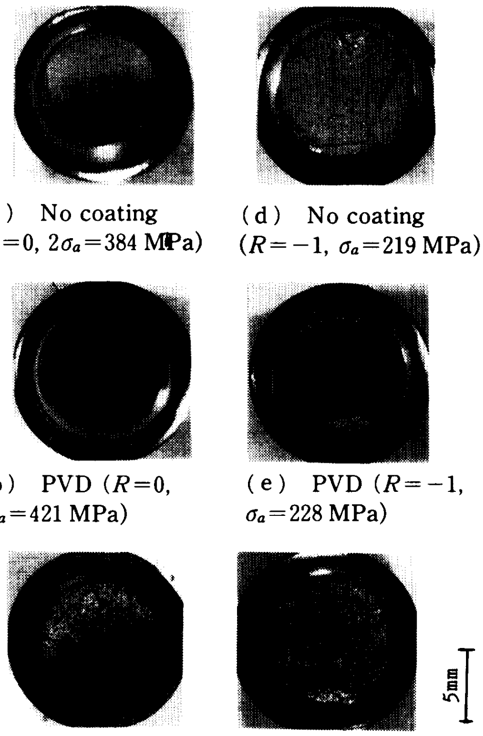

(a) No coating ($R=0$, $2\sigma_a=384$ MPa)
(d) No coating ($R=-1$, $\sigma_a=219$ MPa)
(b) PVD ($R=0$, $2\sigma_a=421$ MPa)
(e) PVD ($R=-1$, $\sigma_a=228$ MPa)
(c) CVD (1 223 K, $R=0$, $2\sigma_a=384$ MPa)
(f) CVD (1 273 K, $R=-1$, $\sigma_a=229$ Mpa)

Fig. 11 Macroscopic observation of fracture surface

3.5 Fractography

Figure 11 shows macroscopic observations of the fracture surface of the tested specimen. Under the condition of decreased fatigue life, the number of ratchet marks on the fracture surface of the coated material, which are the result of multiple fatigue crack origins, is larger than that of the uncoated specimen. On the other hand, this number was less than that of the uncoated specimen, under the condition of increased fatigue life.

Figure 12 shows the relationship between stress amplitude and number of cracks on the fracture surface. The number of cracks on the fracture surface of

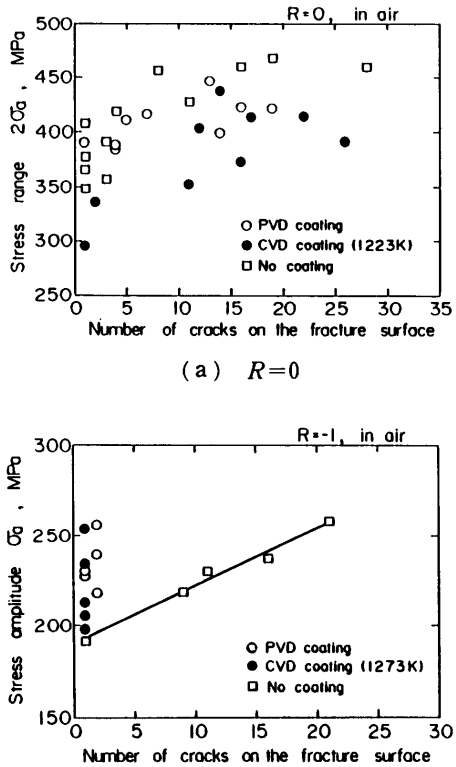

(a) $R=0$
(b) $R=-1$

Fig. 12 Relation between stress amplitude and number of cracks on the fracture surface

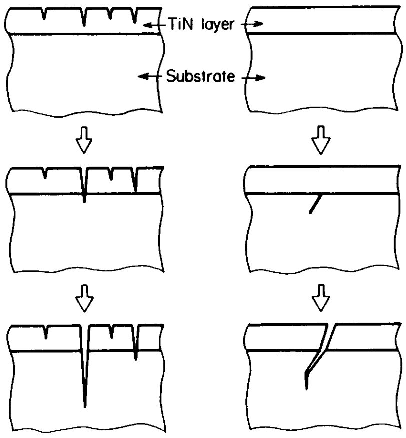

(a) Fatigue strength decrease (b) Fatigue strength increase

Fig. 13 Schematic illustration of crack initiation of TiN-coated material

coated material is larger than that of the uncoated specimens under the testing conditions of a stress ratio of $R=0$ and high stress amplitude level. On the other hand, the number of cracks is less than that of the uncoated specimen, when $R=-1$. It is considered that the number of cracks on the fracture surface is correlated with the fatigue life of the coating film.

3.6 Fatigue crack initiation mechanism of coated material

From the experimental results and discussion, the fatigue crack initiation mechanism of coated material can be summarized as in Fig. 13. Under testing conditions where large deformation occurs or accunulates during fatigue, for example, when $R=0$ and with high stress amplitude, TiN coating film is fractured at an early stage of the fatigue process, because it is too brittle to accommodate the substrate metal. Thus, many cracks may be induced to initiate at the substrate by flaws of the coating film (Fig. 13(a)). On the other hand, under testing conditions without large cyclic deformation of the specimen, crack initiation is delayed by hard coating film on the specimen surface, which can act as a barrier to the egress of dislocations (Fig. 13(b)).

4. Conclusions

The following conclusions were obtained from static tensile tests and fatigue tests under two levels of stress ratio using specimens of carbon steel coated with TiN by PVD and CVD.

(1) Mechanical properties of the coated material were not changed by the coating film. Flaws on the coating film deposited by PVD and CVD occurred at total tensile strains of 0.38% and 0.87%, respectively, under the static tensile test.

(2) The fatigue life of specimens coated by PVD was increased under conditions where $R=0$, except in the region of high stress amplitude. Also, the fatigue life of the specimens coated by CVD under condition where $R=0$ was smaller than that of the uncoated specimens.

(3) Increase in fatigue strength was observed in both PVD- and CVD-coated specimens under condition where $R=-1$, as compared with that of uncoated specimens.

(4) The difference in fatigue life of coated specimens with an applied stress ratio is due to the crack initiation behavior in the substrate induced by the rupture of the coating film.

References

(1) Shiozawa, K. and Ohshima, S., The Effect of TiN Coating on Fatigue Strength of Carbon Steel, J. Soc. Mat. Sci., (in Japanese), Vol. 39, No. 442 (1990), p. 299.

(2) Shiozawa, K. and Ohshima, S., The Effect of TiN Coating on Corrosion Fatigue Strength of Carbon Steel, J. Soc. Mat. Sci., (in Japanese), Vol. 39, No. 442 (1990), p. 958.

(3) Murakami, M., Takeuchi, T., Yano, T. and Katsumura M., Fatigue Properties of TiN Films on Steel Coated by Dynamic Mixing, Mechanical Behaviour of Materials, Vol. 6, (1991), p. 487.

(4) Hashimoto, M., Nagashima, S. and Shiratori, M., An X-Ray on Residual Stress and Fatigue Characteristics of TiC Coated Steels, J. Soc. Mat. Sci., (in Japanese), Vol. 39, No. 437 (1990), p. 150.

(5) Iron and Steel Institute of Japan, D. C. Potential Method of Crack Initiation Detection in High Temperature Low Cycle Fatigue -ISIJ Recommendation-, (1989), p. 9, Iron and Steel Institute of Japan.